Letter

Dynamical systems theory of cellular reprogramming

Yuuki Matsushita, Tetsuhiro S. Hatakeyama ⬤, and Kunihiko Kaneko ⬤*

Department of Basic Science, Graduate School of Arts and Sciences, University of Tokyo, 3-8-1 Komaba, Meguro-ku, Tokyo 153-8902, Japan

In cellular reprogramming, almost all epigenetic memories of differentiated cells are erased by the over-expression of a few genes, resulting in regaining pluripotency, the potential for differentiation. Considering the interplay between oscillatory gene expression and slower epigenetic modifications, such reprogramming is perceived as an unintuitive, global attraction to the unstable manifold of a saddle, which represents pluripotency. The universality of this scheme is confirmed by the repressilator model and by gene regulatory networks that are randomly generated and extracted from embryonic stem cells.

In the development of multicellular organisms, cells with identical genomes differentiate into distinct cell types. This cellular differentiation process has often been picturized as balls falling down the epigenetic landscape, as originally proposed by Waddington [1]: Balls start from the top of the landscape and as development progresses, they fall into distinct valleys corresponding to differentiated cell types. In modern biology, such landscapes are believed to be formed by epigenetic regulation, including DNA and chromatin modifications [2–5]. For pluripotent cells, these modifications are small, whereas each differentiated cell type has a different epigenetic modification pattern [6–9]. Cells with pluripotency, such as embryonic stem (ES) cells, are located in the vicinity of the first branching point into the valleys, because they can easily differentiate into different cell types with only slight stimuli [10].

In 2006, the seminal study by Takahashi and Yamanaka demonstrated that differentiated cells can regain pluripotency only by overexpressing a few genes (the so-called four *Yamanaka factors*). This was termed as reprogramming to form induced pluripotent stem (iPS) cells [11]. Reprogramming is often described as "climbing" the epigenetic landscape [12–14]. However, this hypothesis has a basic issue that needs to be resolved. In the cellular reprogramming reported by Takahashi and Yamanaka and others, only a few genes are overexpressed, without direct manipulation of the epigenetic state, even though the erasure of epigenetic memories is a key factor for cellular reprogramming [12]. In other words, epigenetic memories are erased only by the perturbation of gene expression. Moreover, only a few genes (e.g., four genes) are overexpressed, which are notably fewer than the total number of genes involved. By such simple manipulation, the cellular

state successfully returns to the top of the landscape, which is an unstable point, as it is followed by differentiation. Thus, the following problem in cellular reprogramming needs to be solved: How can reprogramming robustly make cells head toward an "unstable" pluripotent state via the overexpression of only a few genes?

Theoretically, these issues should be resolved based on the dynamical systems theory. The interplay between fast gene regulation and slow epigenetic dynamics shapes the epigenetic landscape, and differentiated cells are represented by different attractors [15–17]. Therefore, upon reprogramming, cellular states starting from different attractors first converge into a unique pluripotent state, which is unstable, followed by their progression toward various attractors. At first glance, these requirements seem incompatible; an unstable state (e.g., repeller) is not attracted from different initial conditions. Therefore, to satisfy these requirements, the pluripotent cell is expected to be represented at least by a saddle that is attracted from many directions and departs only along unstable directions (manifolds), which represent the cell differentiation process, leading to attractors of different destinations. To regain pluripotency by reprogramming, cellular states must be placed on the stable manifold of the saddle by common manipulations from different attractors. However, such manipulation would require fine-tuned control. In contrast, reprogramming is mediated by the overexpression of a few common genes across various differentiated cell types. Therefore, some dynamical systems concept beyond just a saddle is needed.

Recent advances in experiments provide some clues on this subject. Temporal oscillations in gene expression have been reported during cell differentiation and in embryonic stem cells. The relevance of oscillatory expression or dynamic heterogeneity to pluripotency has been noted experimentally [18–25] and theoretically [26–32]. Cell differentiation processes accompanied by loss of pluripotency have been studied in relation with the loss of oscillation [19,26]. The possible relationship between oscillatory cellular dynamics and pluripotency is also observed in cell cycle changes through cellular differentiation [33,34]. Notably, oscillatory

---

*kaneko@complex.c.u-tokyo.ac.jp

dynamics in epigenetic modification (DNA methylation) through the course of cell differentiation have been reported recently [35,36].

Considering the possible significance of oscillatory dynamics, it is natural that the relation between gene expression dynamics and epigenetic modification also plays an important role in cellular reprogramming. Thus, it is reasonable to consider that in the oscillation of fast gene expression around the saddle point of slow epigenetic dynamics, global attraction to it from broad initial conditions may be attained beyond its stable manifold. As the oscillation dynamics are extended beyond the stable manifold of a saddle, global attraction to the vicinity of the saddle may be facilitated by exploiting the interplay between fast gene expression and slow modification dynamics.

In this Letter, we examine this possibility using a dynamical system model with a gene regulatory network (GRN) and epigenetic modification. Although the interplay between gene expression and epigenetic modification is known to be essential to cell differentiation and reprogramming, the molecular details of epigenetic modifications are often so complex that modeling the entire epigenetic modification process is quite difficult. For instance, DNA methylation, one of the popular epigenetic processes, modifies DNA segments, whereas histone modification changes the efficiency of the DNA compaction process [3–5]. Although diverse molecular mechanisms are involved in epigenetic modification, they generally change the feasibility of gene expression. Hence, we adopted a simple "coarse-grained" model that captures this modification in gene expression feasibility to elucidate how the interplay between gene expression dynamics and epigenetic modification leads to cellular differentiation and reprogramming. We adopted reinforcement dynamics, which are inevitably required for a stable heritage of differentiated cell type, wherein the gene expression state is imprinted on the epigenetic state.

We consider a cell model in which the cellular state is represented by the expression x_i and epigenetic modification level θ_i for each gene i, with $i = 1, 2, \ldots, N$. As mentioned above, this set of θ_i values represents the "coarse-grained" epigenetic state. It can correspond to various epigenetic modification levels, such as the DNA methylation level, histone modification level, and chromatin density. Gene expression dynamics, with faster timescales, are governed by GRN with mutual activation or inhibition by transcription factors [37–41], whereas slower epigenetic dynamics change the feasibility of gene expression, which follows gene expression patterns. We assumed the epigenetic feedback reinforcement, meaning that as a gene is expressed more or silenced, the more feasible or harder it is to express, respectively. This hypothesis was based on experimental observations on the Trithorax (TrxG) and Polycomb (PcG) group proteins, which are two essential epigenetic factors for cellular differentiation [42–44]. Specifically, we adopted

$$\frac{dx_i}{dt} = F\left(\sum_j J_{ij}x_j + \theta_i + I_i(t)\right) - x_i, \qquad (1a)$$

$$\frac{d\theta_i}{dt} = \frac{1}{\tau}(x_i - \theta_i). \qquad (1b)$$

In Eq. (1a), gene expression shows an on-off response to the input by adopting the function $F(z) = \tanh(\beta z)$, whereas $\beta = 40$ [45]. If J_{ij} is positive or negative, gene j activates or inhibits gene i, respectively, whereas J_{ij} is set to 0 if no regulation exists. External input $I_i(t)$ is applied only during reprogramming manipulation to flip the expression of the gene i. For simplicity, $I_i(t)$ takes a constant nonzero value when gene i is overexpressed for reprogramming manipulation and is zero otherwise.

In Eq. (1a), $-\theta_i$ functions as a threshold of the expression of gene i, which represents the epigenetic modification status (when there is no epigenetic modification, it takes the value zero). Equation (1b) represents epigenetic feedback regulation. Following the experimental observation of positive epigenetic feedback [46–52], we adopted this simple form as its specific form, which is yet to be confirmed [32,53–55]. Here, τ denotes the characteristic timescale for epigenetic modifications, which is assumed to be sufficiently larger than 1; the change in epigenetic modification is much slower than that of gene regulatory dynamics [56–58].

Recalling the relevance of oscillatory dynamics, we chose a GRN in which oscillatory dynamics were generated for appropriate θ_i values (specifically at $\theta_i \sim 0$). First, we adopted a repressilator model as a minimal model [see Fig. S4(a) [59]], consisting of three genes that repress the expression of the next gene in a cyclic manner [60]. Specifically, we chose $J_{21} = J_{32} = J_{13} = -g = -0.4$ in Eq. (1a).

The expression of x_i in this model showed a limit-cycle oscillation when θ_i was close to zero. Thus, for epigenetic modification to change θ_i following Eq. (1b), the states were differentiated into three fixed-point attractors $\{\theta_1, \theta_2, \theta_3\} = \{-1, 1, 1\}, \{1, -1, 1\}, \{1, 1, -1\}$ [61], after first approaching a straight line $\theta_1 = \theta_2 = \theta_3$, as shown in Fig. 1(a) [62] [see also Fig. S5(a) [59]]. In these fixed points, $dx_i/dt = 0$ and $d\theta_i/dt = 0$ were satisfied, i.e., the differentiation of expression x_i was embedded into the epigenetic modification θ_i.

Next, we considered "reprogramming." Starting from one of the differentiated fixed points, we added external input $I_i(t)$ to again invoke transient oscillation [black dotted line in Fig. 1(b)]. Later, $I_i(t)$ was set to zero. After reprogramming manipulation, they approached a line with $\theta_1 = \theta_2 = \theta_3$ around the origin and then deviated from the line to one of the three fixed points [Fig. 1(b)], in the same manner as the differentiation process. During this reprogramming process, the memory of the differentiated states was erased. Once the oscillation in x was recovered, the approach to the straight line and deviation from it always followed [Fig. 1(c)].

Next, we studied how attraction to the straight line occurs, followed by the progression of differentiation. For this, we considered the adiabatic limit of $\tau \to \infty$. For a fixed θ_i, we first obtained the attractor x_i. Then, the evolution of θ_i was obtained by replacing x_i in Eq. (1b) by its time average $\bar{x}_i$ for a given θ_i, as follows:

$$\frac{d\theta_i}{dt} = \bar{x}_i(\theta_i) - \theta_i (\equiv \Theta_i). \qquad (2)$$

In the three-variable Eq. (2), $\{\theta_1, \theta_2, \theta_3\} = \{0, 0, 0\}$ is a fixed-point solution because $x_i(t)$ shows a symmetric limit-cycle oscillation, such that $\bar{x}_i = 0$ for all i therein for $\{\theta_1, \theta_2, \theta_3\} = \{0, 0, 0\}$. By slightly perturbing θ_i as a parameter, $\bar{x}_j$ changed
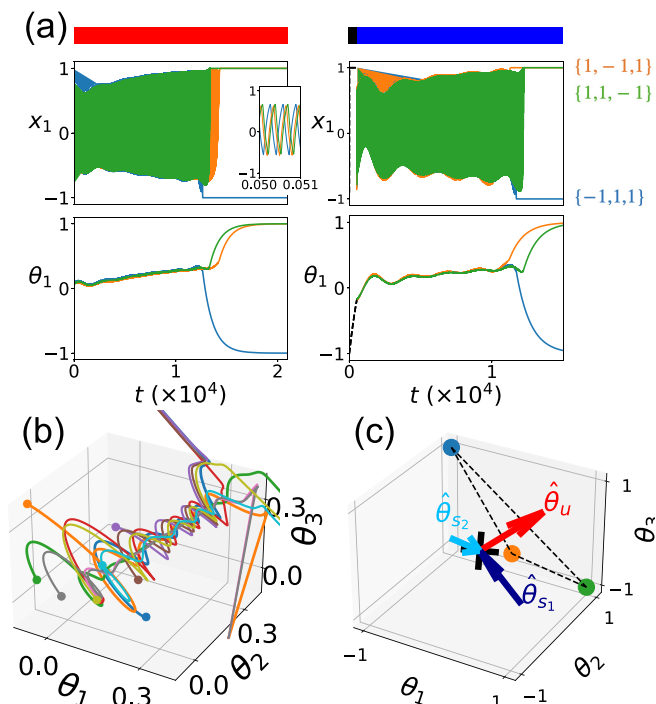
FIG. 1. (a) Cell differentiation and reprogramming of the repressilator model with $\tau = 10^3$. The upper bar indicates differentiation (red), reprogramming manipulation (black), and the subsequent process (blue) without it ($I_i = 0$). We plotted the time development of x_1, θ_1 [see Figs. S5(a) and S5(b) [59] for the time series of all variables]. Left: Three trajectories were sampled from slightly different initial conditions near $\theta_i = 0$. Right: From the fixed point $\{-1, 1, 1\}$, we tested three slightly different time spans to add external input (520, 530, 540). After reprogramming manipulation, the cellular state first approached $\theta_1 = \theta_2 = \theta_3$, and then it differentiated to the three fixed points again. (b) Trajectories through reprogramming and differentiation were plotted in the $(\theta_1, \theta_2, \theta_3)$ space. Ten attempts were overlaid by considering the initial conditions in $x_i \in [-1, 1]$, $\theta_i \in [-0.25, 0.25]$, which allowed oscillation. Attraction toward the straight line $\theta_1 = \theta_2 = \theta_3$ and departure from it was discernible. (c) Eigenvector $\{v_k\}$ and variables $\{\hat{\theta}_k\}$ (see text). The black X mark represents the saddle point at origin $\{0, 0, 0\}$, whereas the three colored points represent the fixed points $\{-1, 1, 1\}$ (blue), $\{1, -1, 1\}$ (orange), and $\{1, 1, -1\}$ (green).

accordingly. From $\partial \bar{x}_i / \partial \theta_j$, we obtained the Jacobi matrix $\partial \Theta_i / \partial \theta_j$ with eigenvalues $\{\lambda_k\}$ and eigenvectors $\{v_k\}$. As shown in Fig. 1(d), the $\{\theta_1, \theta_2, \theta_3\} = \{0, 0, 0\}$ fixed point was a saddle, with the eigenvector $v_u = \{1, 1, 1\}/\sqrt{3}$ corresponding to $\lambda_u > 0$ (unstable axis), and $v_{s_1} = \{2, -1, -1\}/\sqrt{6}$, $v_{s_2} = \{0, -1, 1\}/\sqrt{2}$ for $\text{Re}(\lambda_{s_1}) = \text{Re}(\lambda_{s_2}) < 0$ [see Supplemental Material (SM) Sec. 1A [59]]. To investigate θ dynamics along each of the eigenvectors v_k ($k = u, s_1, s_2$), we introduced the variable $\hat{\theta}_k$, a projection of θ on v_k (i.e., $\hat{\theta}_k = \theta \cdot v_k$, with v_k normalized). Notably, owing to the symmetry of the repressilator, the unstable manifold was in line with the eigenvector v_u (see SM Sec. 1A [59]).

As shown in Figs. 1(c) and 1(d), the straight line to which all trajectories converged agreed with the unstable manifold v_u [Fig. 2(a)]. Of course, attraction to the v_u axis was natural if the initial conditions were restricted onto the stable manifold
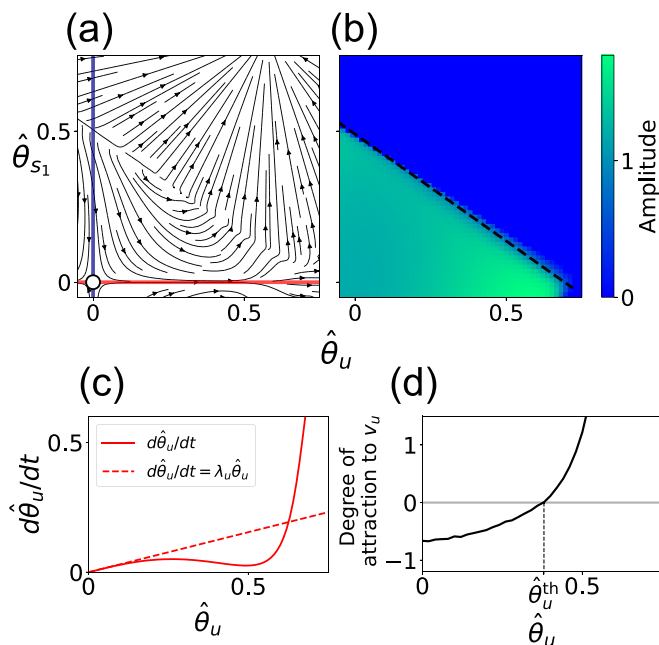

FIG. 2. (a) Stream plot of the $(d\hat{\theta}_u/dt, d\hat{\theta}_{s_1}/dt)$ in $(\hat{\theta}_u, \hat{\theta}_{s_1})$ space according to Eq. (2). The red (blue) line represents the direction of the eigenvector $v_u (v_{s_1})$. (b) Attractor in the x space for each fixed θ value. For the green and blue regions, the attractor in the x space was the limit cycle and fixed point, respectively. (c) $d\hat{\theta}_u/dt$ plotted as a function of $\hat{\theta}_u$. For comparison, we plotted $d\hat{\theta}_u/dt = \lambda_u \hat{\theta}_u$ (red dotted line). (d) Degree of attraction to v_u. ν, in the text, is plotted as a function of $\hat{\theta}_u$. If it was negative or positive, $\{\theta\}$ was attracted to or had departed from v_u, respectively. See Fig. S6 [59] for more details.

for $\{\theta_1, \theta_2, \theta_3\} = \{0, 0, 0\}$. However, we observed attraction toward the unstable axis over a wide range of initial conditions for $\{\theta_i\}$, supporting the oscillation of x_i. Furthermore, the magnitudes of eigenvalues for the stable and unstable eigenvectors were of the same order $[\text{Re}(\lambda_u) = 0.31, \text{Re}(\lambda_{s_1}) = \text{Re}(\lambda_{s_2}) = -0.66$, see Fig. S5(c) [59]]. Thus, the reprogramming dynamics shown in Fig. 1(b) could not be explained only by linear stability.

To elucidate whether the nonlinear effect suppresses instability along the v_u axis, we computed $d\hat{\theta}_u/dt$. As shown in Fig. 2(c), $d\hat{\theta}_u/dt$ was drastically reduced from that in the linear case. We also computed $(d\hat{\theta}_{s_1}/dt, d\hat{\theta}_{s_2}/dt)$ for a certain $\hat{\theta}_u$ value [i.e., the flow structure in the $(\hat{\theta}_{s_1}, \hat{\theta}_{s_2})$ plane, sliced along the $\hat{\theta}_u$ axis], which showed that $\hat{\theta}_{s_1} = 0$ changed from stable to unstable at $\hat{\theta}_u = \hat{\theta}_u^{\text{th}}$ (~ 0.4) [see Figs. 2(d) and S6 [59]]. Up to $\hat{\theta}_u < \hat{\theta}_u^{\text{th}}$ (~ 0.4), θ_i in the $(\hat{\theta}_{s_1}, \hat{\theta}_{s_2})$ plane was attracted to the $\hat{\theta}_u$ axis. By further increasing $\hat{\theta}_u$ beyond $\hat{\theta}_u^{\text{th}}$, θ_i departed from the $\hat{\theta}_u$ axis rotating in the $(\hat{\theta}_{s_1}, \hat{\theta}_{s_2})$ plane, leading to differentiation toward three distinct fixed points.

To understand how slow motion along $\hat{\theta}_u$ and attraction to $\hat{\theta}_u$ occurred, we first fixed θ_i and studied the change in the x attractor, as shown in Fig. 2(b). In the green and blue region, the x attractor was a limit cycle and fixed point, respectively, for $(\hat{\theta}_u, \hat{\theta}_{s_1})$. At the line $\hat{\theta}_{s_1} = -\hat{\theta}_u/\sqrt{2} + \sqrt{6}/5$ (as discussed in SM Secs. 1B and 1C [59]), x dynamics exhibited bifurcation from the limit cycle to a fixed point $\{1, -1, 1\}$ (see Fig. S7 [59] for more details). Considering the symmetry of the repressilator, bifurcations to three
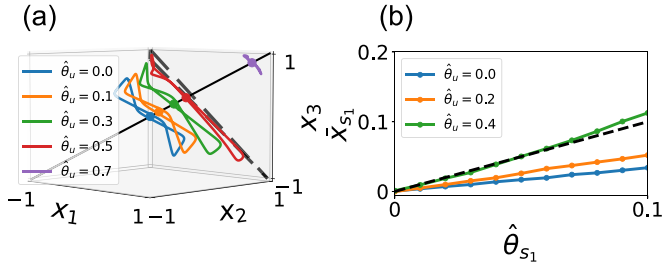
FIG. 3. (a) Change in the limit cycle $x(t)$ (solid line) and $\bar{x}$ (point) along $\hat{\theta}_u$. The black dotted line shows an equilateral triangle with corners $\{-1, 1, 1\}, \{1, -1, 1\}, \{1, 1, -1\}$ (see SM Sec. 1D [59]). (b) $\bar{x}_{s_1}$ as a function of $\hat{\theta}_{s_1}$. The slope of each line corresponds to $\partial \bar{x}_{s_1}/\partial \hat{\theta}_{s_1}$ for $\hat{\theta}_u$. From $\partial \Theta_{s_1}/d\hat{\theta}_{s_1}$, if the slope is less than one, the orbits are attracted toward $\hat{\theta}_u$. For comparison, we plotted $\bar{x}_{s_1} = \hat{\theta}_{s_1}$ as a black dotted line. At $\hat{\theta}_u \sim 0.4$, $\partial \bar{x}_{s_1}/\partial \hat{\theta}_{s_1}$ exceeds one.

fixed points $\{-1, 1, 1\}, \{1, -1, 1\}, \{1, 1, -1\}$ coexisted in the $(\hat{\theta}_{s_1}, \hat{\theta}_{s_2})$ plane. With the increase in $\hat{\theta}_u$, the limit cycle approached the three fixed points.

Next, we discuss the mechanism of slow motion along $\hat{\theta}_u$. From Eq. (2), movement along $\boldsymbol{v}_u$ followed $d\hat{\theta}_u/dt = \bar{x}_u(\hat{\theta}_u) - \hat{\theta}_u$ (we defined x_k as a projection on $\boldsymbol{v}_k$). As shown in Fig. 3(a), the limit cycle approached the plane spanned by the three fixed points $\{-1, 1, 1\}, \{1, -1, 1\}, \{1, 1, -1\}$ as $\hat{\theta}_u$ increased. In the plane, $\bar{x}_u$ comprised $1/\sqrt{3}$, and θ_i increased following Eq. (2) (see SM Sec. 1D [59] for more details). Then, as $\hat{\theta}_u$ approaches $1/\sqrt{3}$, $d\hat{\theta}_u/dt$ was minimized, as shown in Fig. 2(c).

Next, we considered how attraction to the $\boldsymbol{v}_u$ from the $(\hat{\theta}_{s_1}, \hat{\theta}_{s_2})$ plane was lost at the $\hat{\theta}_u = \hat{\theta}_u^{\text{th}}$. By considering $\hat{\theta}_u$ as a parameter, the direction of flow in the $(\hat{\theta}_{s_1}, \hat{\theta}_{s_2})$ plane toward the $\boldsymbol{v}_u$ was determined by the sign of $\partial \Theta_{s_1}/\partial \hat{\theta}_{s_1} = \partial \bar{x}_{s_1}/\partial \hat{\theta}_{s_1} - 1 \equiv \nu \Theta_{s_1}$ (we defined Θ_{s_1} as a projection on $\boldsymbol{v}_{s_1}$). As shown in Fig. 2(b), with the increase in $\hat{\theta}_u$, the bifurcation point from the limit cycle to the fixed point approached the $\hat{\theta}_u = 0$ line. Hence, by slightly changing $\hat{\theta}_{s_1}$, $\bar{x}$ reached fixed points. Accordingly, $\partial \bar{x}_{s_1}/\partial \hat{\theta}_{s_1}$ increased beyond one, so that $\partial \Theta_{s_1}/\partial \hat{\theta}_{s_1}$ became positive at $\hat{\theta}_u$, approaching $\hat{\theta}_u^{\text{th}} \sim 0.4$, as shown in Figs. 2(d) and 3(b).

Thus, we unveiled how attraction to the unstable manifold is achieved by slow epigenetic fixation of the oscillation of fast gene expression in the repressilator model. Following this picture, reprogramming is possible by forcing the cells to return to the oscillatory state. Then, the cell is attracted to a pluripotent state with low epigenetic modification $\theta_i \sim 0$, followed by differentiation to distinct cell types with specific θ values. Notably, the differentiation process [63], as well as the present reprogramming process, is robust against internal or external noise because the initial pluripotent state is globally attracted (see Fig. S8 [59]) [64].

To verify the generality of this reprogramming scheme, we examined several GRN models with more degrees of freedom. As discussed in Ref. [63], differentiation from oscillatory states is often observed in GRNs (e.g., 20% of randomly generated GRNs show oscillatory dynamics for $N = 10$). An example is shown in Fig. S9(a) [59]. From a differentiated state, we overexpressed three genes to regain oscillatory expression [black line in Fig. S9(a) [59]]. Later, global attraction
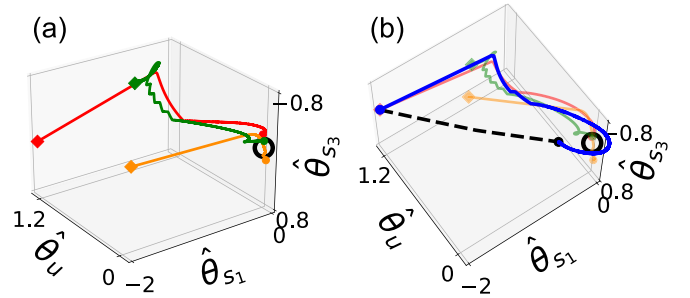

FIG. 4. (a) Cell differentiation and (b) reprogramming in the five-gene model (a) Three orbits starting from the vicinity of the saddle point $\theta_i = 0$ for all i (black dotted point), reached three distinct cell types. (b) From differentiated cell types (red point), we added the external input $I_i(t)$ to Nanog, Oct4, and Klf4 for a certain time span (black dotted line). After such reprogramming manipulation, we set $I_i(t) = 0$. The cell state then spontaneously approached the saddle point and then reinitiated the progression of differentiation (blue line). $\tau = 10^3$. See Fig. S10 [59] for more details.

to the unstable manifold also occurred as discussed above. The cell states then branched again to distinct fixed point states [blue line in Fig. S9(a) [59]]. In these cases, the original pluripotent state with $\theta = 0$ was an unstable fixed point, with one positive eigenvalue for the Jacobi matrix of θ dynamics [Fig. S9(d) [59]], as in the repressilator model. Even though the degrees of freedom increased, the unstable manifold was one dimensional, and attraction to the manifold occurred from a higher-dimensional state space. This implies that reprogramming manipulation requires only partial degrees of freedom compared with the total number of genes. In fact, overexpression of three genes is sufficient for reprogramming in GRN models with $N = 10$, as far as we have investigated.

The present mechanism also works in a model extracted from the GRN of an embryonic stem cell [65], as a core network with five genes (*Nanog, Oct4, Gata6, Gata4,* and *Klf4*) [32] [see Fig. S4(b)] [66]. *Oct4, Sox2,* and *Klf4* are known as factors to induce reprogramming. The model involves a negative feedback loop, as in the repressilator, in addition to positive feedback regulation. In this five-gene model, x_i and θ_i oscillate in the region near the origin, and then differentiation to three fixed points progresses as in the case of the repressilator [three lines in Fig. 4(a)], whereas $\theta_i = 0$ for all i represents a saddle point with one unstable manifold and four stable manifolds, as shown in Fig. S10(b). After overexpression of *Oct4*, *Nanog*, and *Klf4* from one of the differentiated cell types for a certain time span [black dotted line in Fig. 4(b)] [67], the epigenetic state θ_i approaches the unstable manifold for the unstable fixed point $\theta_i = 0$, leading to the recovery of pluripotency [blue line in Fig. 4(b)].

In this Letter, we have shown that oscillatory gene expression dynamics with slow epigenetic modifications lead to cellular reprogramming by the overexpression of only a few genes. Global attraction to the unstable manifold of the saddle point explains the reprogramming process. Now, the return to the top of the landscape by reprogramming, which is seemingly unstable, is explained by the strong attraction toward the unstable manifold of the saddle, and its suppressed instability

along with the unstable manifold, owing to the approach of the limit cycle of bifurcation to the fixed points. The memory of the cellular state before reprogramming manipulation was erased through this reprogramming process.

According to the present study, regaining oscillation is the main requirement for reprogramming and elaborate manipulation to induce cells into a specific state is not necessary. This explains the role of oscillations in the gene expression in pluripotent cells [19] and epigenetic modification through the differentiation process [35]. It also explains how reprogramming is possible by overexpressing only a few genes among thousands [11,14]. Timescale separation between the fast expression dynamics and slow epigenetic modification feedback required is also consistent with observations of previous studies [56,57].

If we treat slowly varying θ_i values as parameters, our model could be represented by a gene expression dynamical system with external bifurcation parameters θ_i, as also discussed, for instance, in Ref. [68]. However, in developmental processes, the epigenetic state changes slowly and autonomously depending on the gene expression state, as elucidated in the current study. It will thus be important to make a general formulation for such slow-fast dynamical systems [69,70].

Although there are some experimental reports on oscillation in gene expression [23] and epigenetic modification during cellular differentiation, such as reports on DNA methylation levels [35] and chromatin compaction states [71], it is further important to elucidate the role of such oscillation in epigenetic modifications to differentiation and reprogramming, by measuring its time course under controlled conditions. Our theory suggests that through cellular reprogramming, the epigenetic state will first converge to a common state from differentiated cell types, with transient oscillation. The genes to be overexpressed for reprogramming (e.g., the Yamanaka factor) will then be those needed to recover oscillation in gene expression dynamics.

[1] C. Waddington, *The Strategy of the Genes* (George Allen & Unwin, London, 1957).

[2] A. Bird, Perceptions of epigenetics, Nature (London) **447**, 396 (2007).

[3] A. D. Goldberg, C. D. Allis, and E. Bernstein, Epigenetics: A landscape takes shape, Cell **128**, 635 (2007).

[4] R. Cortini, M. Barbi, B. R. Caré, C. Lavelle, A. Lesne, J. Mozziconacci, and J.-M. Victor, The physics of epigenetics, Rev. Mod. Phys. **88**, 025002 (2016).

[5] M. A. Surani, K. Hayashi, and P. Hajkova, Genetic and epigenetic regulators of pluripotency, Cell **128**, 747 (2007).

[6] E. Meshorer, D. Yellajoshula, E. George, P. J. Scambler, D. T. Brown, and T. Misteli, Hyperdynamic plasticity of chromatin proteins in pluripotent embryonic stem cells, Dev. Cell **10**, 105 (2006).

[7] Y. Atlasi and H. G. Stunnenberg, The interplay of epigenetic marks during stem cell dierentiation and development, Nat. Rev. Genet. **18**, 643 (2017).

[8] T. S. Mikkelsen, M. Ku, D. B. Jaffe, B. Issac, E. Lieberman, G. Giannoukos, P. Alvarez, W. Brockman, T.-K. Kim, R. P. Koche *et al.*, Genome-wide maps of chromatin state in pluripotent and lineage-committed cells, Nature (London) **448**, 553 (2007).

[9] K. Tripathi and G. I. Menon, Chromatin Compaction, Auxeticity, and the Epigenetic Landscape of Stem Cells, Phys. Rev. X **9**, 041020 (2019).

[10] S. Levenberg, J. S. Golub, M. Amit, J. Itskovitz-Eldor, and R. Langer, Endothelial cells derived from human embryonic stem cells, Proc. Natl. Acad. Sci. USA **99**, 4391 (2002).

[11] K. Takahashi and S. Yamanaka, Induction of pluripotent stem cells from mouse embryonic and adult fibroblast cultures by defined factors, Cell **126**, 663 (2006).

[12] K. Takahashi and S. Yamanaka, A decade of transcription factor-mediated reprogramming to pluripotency, Nat. Rev. Mol. Cell Biol. **17**, 183 (2016).

[13] K. Hochedlinger and K. Plath, Epigenetic reprogramming and induced pluripotency, Development **136**, 509 (2009).

[14] S. Velychko, K. Adachi, K.-P. Kim, Y. Hou, C. M. MacCarthy, G. Wu, and H. R. Schöler, Excluding Oct4 from Yamanaka Cocktail unleashes the developmental potential of iPSCs, Cell Stem Cell **25**, 737 (2019).

[15] S. A. Kauffman, Metabolic stability and epigenesis in randomly constructed genetic nets, J. Theor. Biol. **22**, 437 (1969).

[16] J. Wang, L. Xu, E. Wang, and S. Huang, The potential landscape of genetic circuits imposes the arrow of time in stem cell dierentiation, Biophys. J. **99**, 29 (2010).

[17] G. Forgacs and S. A. Newman, *Biological Physics of the Developing Embryo* (Cambridge University Press, Cambridge, UK, 2005).

[18] I. Palmeirim, D. Henrique, D. Ish-Horowicz, and O. Pourquié, Avian hairy gene expression identifies a molecular clock linked to vertebrate segmentation and somitogenesis, Cell **91**, 639 (1997).

[19] T. Kobayashi, H. Mizuno, I. Imayoshi, C. Furusawa, K. Shirahige, and R. Kageyama, The cyclic gene *Hes1* contributes to diverse differentiation responses of embryonic stem cells, Genes Dev. **23**, 1870 (2009).

[20] M. A. Canham, A. A. Sharov, M. S. Ko, and J. M. Brickman, Functional heterogeneity of embryonic stem cells revealed through translational amplification of an early endodermal transcript, PLoS Biol. **8**, e1000379 (2010).

[21] A. M. Arias and J. M. Brickman, Gene expression heterogeneities in embryonic stem cell populations: Origin and function, Curr. Opin. Cell Biol. **23**, 650 (2011).

[22] K. B. Halpern, S. Tanami, S. Landen, M. Chapal, L. Szlak, A. Hutzler, A. Nizhberg, and S. Itzkovitz, Bursty gene expression in the intact mammalian liver, Mol. Cell **58**, 147 (2015).

[23] J. Zhang, Q. Nie, and T. Zhou, Revealing dynamic mechanisms of cell fate decisions from single-cell transcriptomic data, Front. Genet. **10**, 1280 (2019).

[24] E. Marinopoulou, V. Biga, N. Sabherwal, A. Miller, J. Desai, A. D. Adamson, and N. Papalopulu, Hes1 protein oscillations are necessary for neural stem cells to exit from quiescence, iScience **24**, 103198 (2021).

[25] Y. Zhang, I. Lahmann, K. Baum, H. Shimojo, P. Mourikis, J. Wolf, R. Kageyama, and C. Birchmeier, Oscillations of delta-like1 regulate the balance between dierentiation and maintenance of muscle stem cells, Nat. Commun. **12**, 1318 (2021).

[26] C. Furusawa and K. Kaneko, A dynamical-systems view of stem cell biology, Science **338**, 215 (2012).

[27] E. Ullner, A. Koseska, J. Kurths, E. Volkov, H. Kantz, and J. García-Ojalvo, Multistability of synthetic genetic networks with repressive cell-to-cell communication, Phys. Rev. E **78**, 031904 (2008).

[28] A. Koseska, E. Ullner, E. Volkov, J. Kurths, and J. García-Ojalvo, Cooperative differentiation through clustering in multicellular populations, J. Theor. Biol. **263**, 189 (2010).

[29] N. Suzuki, C. Furusawa, and K. Kaneko, Oscillatory protein expression dynamics endows stem cells with robust differentiation potential, PLoS ONE **6**, e27232 (2011).

[30] A. Koseska, E. Volkov, and J. Kurths, Transition from Amplitude to Oscillation Death Via Turing Bifurcation, Phys. Rev. Lett. **111**, 024103 (2013).

[31] Y. Goto and K. Kaneko, Minimal model for stem-cell differentiation, Phys. Rev. E **88**, 032718 (2013).

[32] T. Miyamoto, C. Furusawa, and K. Kaneko, Pluripotency, differentiation, and reprogramming: A gene expression dynamics model with epigenetic feedback regulation, PLoS Comput. Biol. **11**, e1004476 (2015).

[33] S. Pauklin and L. Vallier, The cell-cycle state of stem cells determines cell fate propensity, Cell **155**, 135 (2013).

[34] A. Soufi and S. Dalton, Cycling through developmental decisions: how cell cycle dynamics control pluripotency, dierentiation and reprogramming, Development **143**, 4301 (2016).

[35] S. Rulands, H. J. Lee, S. J. Clark, C. Angermueller, S. A. Smallwood, F. Krueger, H. Mohammed, W. Dean, J. Nichols, P. Rugg-Gunn *et al.*, Genome-scale oscillations in dna methylation during exit from pluripotency, Cell Syst. **7**, 63 (2018).

[36] S. Kangaspeska, B. Stride, R. Métivier, M. Polycarpou-Schwarz, D. Ibberson, R. P. Carmouche, V. Benes, F. Gannon, and G. Reid, Transient cyclical methylation of promoter DNA, Nature (London) **452**, 112 (2008).

[37] E. Mjolsness, D. H. Sharp, and J. Reinitz, A connectionist model of development, J. Theor. Biol. **152**, 429 (1991).

[38] I. Salazar-Ciudad, J. Garcia-Fernández, and R. V. Solé, Gene networks capable of pattern formation: From induction to reaction–diffusion, J. Theor. Biol. **205**, 587 (2000).

[39] I. Salazar-Ciudad, S. Newman, and R. Solé, Phenotypic and dynamical transitions in model genetic networks I. Emergence of patterns and genotype-phenotype relationships, Evol. Dev. **3**, 84 (2001).

[40] S. Huang, G. Eichler, YaneerBar-Yam, and D. E. Ingber, Cell Fates as High-Dimensional Attractor States of a Complex Gene Regulatory Network, Phys. Rev. Lett. **94**, 128701 (2005).

[41] K. Kaneko, Evolution of robustness to noise and mutation in gene expression dynamics, PLoS ONE **2**, e434 (2007).

[42] R. S. Illingworth, J. J. Hölzenspies, F. V. Roske, W. A. Bickmore, and J. M. Brickman, Polycomb enables primitive endoderm lineage priming in embryonic stem cells, eLife **5**, e14926 (2016).

[43] M. I. Kuroda, H. Kang, S. De, and J. A. Kassis, Dynamic competition of polycomb and trithorax in transcriptional programming, Annu. Rev. Biochem. **89**, 235 (2020).

[44] G. J. Hickey, C. L. Wike, X. Nie, Y. Guo, M. Tan, P. J. Murphy, and B. R. Cairns, Establishment of developmental gene silencing by ordered polycomb complex recruitment in early zebrafish embryos, eLife **11**, e67738 (2022).

[45] Although we adopted a symmetric function, the result to be discussed would not have changed if asymmetric functions, including the Hill function, were introduced.

[46] S. Hihara, C.-G. Pack, K. Kaizu, T. Tani, T. Hanafusa, T. Nozaki, S. Takemoto, T. Yoshimi, H. Yokota, N. Imamoto *et al.*, Local nucleosome dynamics facilitate chromatin accessibility in living mammalian cells, Cell Rep. **2**, 1645 (2012).

[47] M. Grunstein, Yeast heterochromatin: Regulation of its assembly and inheritance by histones, Cell **93**, 325 (1998).

[48] S. L. Schreiber and B. E. Bernstein, Signaling network model of chromatin, Cell **111**, 771 (2002).

[49] I. B. Dodd, M. A. Micheelsen, K. Sneppen, and G. Thon, Theoretical analysis of epigenetic cell memory by nucleosome modification, Cell **129**, 813 (2007).

[50] K. Sneppen, M. A. Micheelsen, and I. B. Dodd, Ultrasensitive gene regulation by positive feedback loops in nucleosome modification, Mol. Syst. Biol. **4**, 182 (2008).

[51] A. Angel, J. Song, C. Dean, and M. Howard, A polycomb-based switch underlying quantitative epigenetic memory, Nature (London) **476**, 105 (2011).

[52] J. C. Spainhour, H. S. Lim, S. V. Yi, and P. Qiu, Correlation patterns between DNA methylation and gene expression in the cancer genome atlas, Cancer Inf. **18** (2019).

[53] C. Furusawa and K. Kaneko, Epigenetic feedback regulation accelerates adaptation and evolution, PLoS ONE **8**, e61251 (2013).

[54] S. Gombar, T. MacCarthy, and A. Bergman, Epigenetics decouples mutational from environmental robustness. did it also facilitate multicellularity? PLoS Comput. Biol. **10**, e1003450 (2014).

[55] B. Huang, M. Lu, M. Galbraith, H. Levine, J. N. Onuchic, and D. Jia, Decoding the mechanisms underlying cell-fate decision-making during stem cell dierentiation by random circuit perturbation, J. R. Soc. Interface **17**, 20200500 (2020).

[56] T. K. Barth and A. Imhof, Fast signals and slow marks: The dynamics of histone modifications, Trends Biochem. Sci. **35**, 618 (2010).

[57] K. Maeshima, K. Kaizu, S. Tamura, T. Nozaki, T. Kokubo, and K. Takahashi, The physical size of transcription factors is key to transcriptional regulation in chromatin domains, J. Phys.: Condens. Matter **27**, 064116 (2015).

[58] M. Sasai, Y. Kawabata, K. Makishi, K. Itoh, and T. P. Terada, Time scales in epigenetic dynamics and phenotypic heterogeneity of embryonic stem cells, PLoS Comput. Biol. **9**, e1003380 (2013).

[59] See Supplemental Material at http://link.aps.org/supplemental/10.1103/PhysRevResearch.4.L022008 for derivations, detailed discussions, and figures.

[60] M. B. Elowitz and S. Leibler, A synthetic oscillatory network of transcriptional regulators, Nature (London) **403**, 335 (2000).

[61] Here, we can approximate the θ_i value of three fixed points to 1 or -1, as we use a sufficiently large value of β ($=40$).

[62] Considering positive/negative symmetry, six attractors exist in the whole space. In this Letter, we only considered the side $\sum \theta_i > 0$.

[63] Y. Matsushita and K. Kaneko, Homeorhesis in Waddington's landscape by epigenetic feedback regulation, Phys. Rev. Research **2**, 023083 (2020).

[64] Thus, one may suspect that the reprogramming efficiency is rather low. However, this limitation could be due to technical problems in experiments for the efficient overexpression of genes. In fact, this efficiency has been increasing through advances in experimental techniques [72,73].

[65] S.-J. Dunn, G. Martello, B. Yordanov, S. Emmott, and A. Smith, Defining an essential transcription factor program for naive pluripotency, Science **344**, 1156 (2014).

[66] In the previous work [32], a specific five-gene model with a complicated epigenetic process and cell-cell interaction was numerically studied to indicate reprogramming is possible by the overexpression of Yamanaka factors. Thus, neither analysis nor elucidation for a general mechanism for reprogramming was available. However, the present Letter presents the mechanism for cellular reprogramming as a result of the global attraction toward the pluripotent state, based on the dynamical systems theory for fast gene expression dynamics and slower epigenetic modification.

[67] *Sox2* is reduced into Nanog in the five-gene model.

[68] D. A. Rand, A. Raju, M. Sáez, F. Corson, and E. D. Siggia, Geometry of gene regulatory dynamics, Proc. Natl. Acad. Sci. USA **118**, e2109729118(2021).

[69] H. Aoki and K. Kaneko, Slow Stochastic Switching by Collective Chaos of Fast Elements, Phys. Rev. Lett. **111**, 144102 (2013).

[70] C. Kuehn, *Multiple Time Scale Dynamics*, Applied Mathematical Sciences Vol. 191 (Springer, Cham, 2015).

[71] B. Roy, L. Yuan, Y. Lee, A. Bharti, A. Mitra, and G. Shivashankar, Fibroblast rejuvenation by mechanical reprogramming and redifferentiation, Proc. Natl. Acad. Sci. USA **117**, 10131 (2020).

[72] Y. Zhao, X. Yin, H. Qin, F. Zhu, H. Liu, W. Yang, Q. Zhang, C. Xiang, P. Hou, Z. Song *et al.*, Two supporting factors greatly improve the efficiency of human ipsc generation, Cell Stem Cell **3**, 475 (2008).

[73] A. Kunitomi, S. Yuasa, F. Sugiyama, Y. Saito, T. Seki, D. Kusumoto, S. Kashimura, M. Takei, S. Tohyama, H. Hashimoto *et al.*, H1foo has a pivotal role in qualifying induced pluripotent stem cells, Stem Cell Rep. **6**, 825 (2016).